Electrochemical and Molecular Assessment of Quinones as CO_2-Binding Redox Molecules for Carbon Capture

Fritz Simeon[1], Michael C. Stern[1], Kyle M. Diederichsen[1], Yayuan Liu[1], Howard J. Herzog[2], T. Alan Hatton[*,1]

[1]Department of Chemical Engineering, Massachusetts Institute of Technology, 77 Massachusetts Avenue, Cambridge, MA 02139, USA.

[2]MIT Energy Initiative, Massachusetts Institute of Technology, 77 Massachusetts Avenue, Cambridge, MA 02139, USA.

KEYWORDS: Carbon dioxide, separation, electrochemistry, redox, quinone.

ABSTRACT: The complexation and decomplexation of CO_2 with a series of quinones of different basicity during electrochemical cycling in dimethylformamide solutions were studied systematically by cyclic voltammetry. In the absence of CO_2, all quinones exhibited two well-separated reduction waves. For weakly complexing quinones, a positive shift in the second reduction wave was observed in the presence of CO_2, corresponding to the dianion quinone-CO_2 complex formation. The peak position and peak height of the first reduction wave was unchanged, indicating no formation of complexes between the semiquinones and CO_2. The relative heights of both reduction waves remained constant. In the case of strongly complexing quinones, the second reduction wave disappeared while the peak height of the first reduction wave approximately doubled, indicating that the two electrons transferred simultaneously at this potential. The observed voltammograms were rationalized through several equilibrium arguments. Both weakly and strongly complexing quinones underwent either *stepwise* or *concerted* mechanisms of oxidation and CO_2 dissociation depending on the sweep rate in the cyclic voltammetric experiments. Relative to *stepwise* oxidation, the *concerted* process requires a more positive electrode potential to remove the electron from the carbonate complexes to release CO_2 and regenerate the quinone. For weakly complexing quinones, the *stepwise* process corresponds to oxidation of the uncomplexed dianion and accompanying equilibrium shift, while for strongly complexing quinones the *stepwise* process would correspond to the oxidation of mono(carbonate) dianion to the complexed semiquinone and accompanying equilibrium shift. This study provides a mechanistic interpretation of the interactions that lead to the formation of quinone-CO_2 complexes required for the potential development of an energy efficient electrochemical separation process and discusses important considerations for practical implementation of CO_2 capture in the presence of oxygen with lower vapor pressure solvents.

Anthropogenic carbon dioxide (CO_2) in the Earth's atmosphere has been cited as a primary cause of global climate change and threatens global public health and welfare. Carbon Capture and Sequestration (CCS) is a necessary element of CO_2 emission abatement strategies intended to meet the goals of the Paris Climate Accord. Major CCS efforts to date have focused on the removal of CO_2 directly from large-scale carbon emitters and storing it in secure geologic reservoirs. Thermal-swing operations using aqueous base scrubbing followed by stripping at elevated temperature have been the chemical sorption processes most investigated over the past two decades for CO_2 capture.[1] Thermal-swing absorption systems, however, have been unable to achieve low enough energy consumption and cost for widespread deployment. Efficiency improvements and cost reductions are currently required for CCS to become cost competitive with other carbon sequestration methods, such as reforestation and soil carbon sequestration.

Electrochemically mediated separations offer a nearly isothermal alternative to the thermal-swing separation strategies typically used for CO_2 capture.[2–5] The driving force in these systems is supplied by a gradient in electric potential, which can be supplied by renewable sources and requires substantially less energy than a thermal system as they are not limited by the Carnot efficiency of temperature swing systems. In 1989, Wrighton and Mizen discovered that the electrode reduction of quinones in the presence of CO_2 results in bis(carbonate) formation, and that upon oxidation the quinones and CO_2 are regenerated.[6] The reversible reductive addition of CO_2 to quinones was subsequently proposed by DuBois *et al*. as a basic concept for electrochemical CO_2 concentrators.[7] Scovazzo *et al*. demonstrated the idea in 2003 by capturing CO_2 from a dilute gas stream and concentrating the gas to atmospheric pressure in a batch electrochemical cell.[8] Despite the encouraging proof-of-concept demonstration under ambient conditions, the quinone electrochemical separator reported by Scovazzo et al. has high-energy consumption with poor efficiency. Our recent study used a poly(1,4-anthraquinone)-carbon nanotube composite as a solid sorbent and successfully demonstrated an electro-swing-based CO_2 separation in a cyclic reactor configuration.[9] Our group has additionally examined quinones in ionic liquids and salt-concentrated aqueous media for CO_2 separations.[10,11] An energy assessment of electrochemical separators

suggests that effective control of the potential can minimize the irreversibility associated with the process.[12]

Quinones are naturally occurring molecules that facilitate biological electron transfer reactions in many cellular respiration and photosynthesis cycles. They are the classical example of organic redox systems and their electrochemistry has been systematically investigated. In dry, aprotic electrolyte solutions, quinones show two consecutive single-electron transfers, separated by about 0.7 V, which correspond to the formation of semiquinones and dianion quinones, respectively.[13] The first electron transfer, associated with the quinone-semiquinone pair, is generally reversible, while the semiquinone-dianion quinone pair formation is quasi-reversible in terms of electron transfer. In aqueous systems, the dianion quinone is protonated readily to form hydroquinone molecules. The fascinating electrochemistry of quinones in aprotic electrolytes on the addition of proton donors has been investigated owing to its natural occurrence in many key biological functions.[14–16] Hydrogen bonding stabilization by weak proton donors shifts positively the reduction potential of the two electron transfer processes with a stronger shift observed on the second wave. Strong proton donors protonate the reduced quinones as indicated by the merging of the two reduction waves and, in some cases, a new pair of reduction and oxidation waves appears at more positive electrode potentials. Intermolecular stabilization of proton donors by hydrogen-bonding interactions results in no loss of reversibility of the first and second electron transfer processes, while protonation of reduced quinones results in irreversible electron transfer. Formation of the O-H bond delocalizes the electronic charge on the oxyanions and results in a higher energy requirement for oxidation of the protonated oxyanions, and hence higher oxidation potentials. The reductive addition of CO_2 to a few quinones has been reported previously;[6,17–23] however a systematic study of quinones for their applicability in carbon capture has not been completed. While it is also of great interest to evaluate the reductive addition of other acidic gases to quinones, such as sulfur oxides, this falls beyond the scope of this paper.

We present here a systematic study of quinone electrochemistry using cyclic voltammetry to probe the reductive addition of CO_2 to quinones to assist in identifying suitable redox-active molecules for electrochemical CO_2 separations. The effect of CO_2 on the electron transfer processes was assessed for a wide range of *para*-quinone structures, including benzoquinone, *para*-naphthoquinone and anthraquinone, and of *ortho*-quinone structures, such as *ortho*-naphthoquinone.

Results and Discussion

Electrochemistry of quinones in dry aprotic electrolyte solutions under an N_2 atmosphere

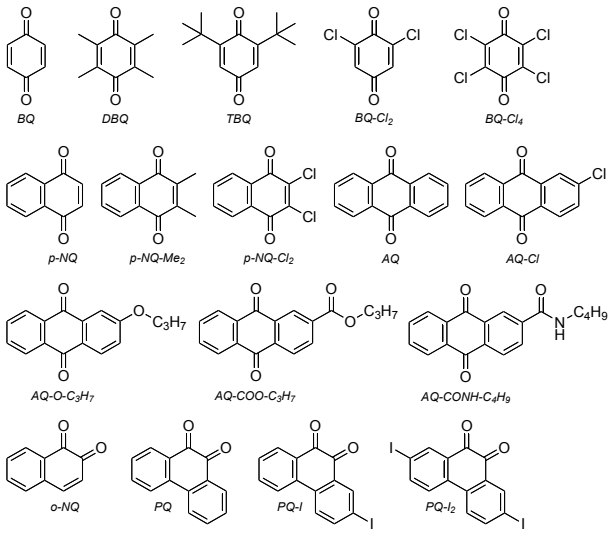

Scheme 1: Molecular structures of various quinones used in this study: *p*-benzoquinone (BQ), tetramethyl-*p*-benzoquinone (DBQ), 2,7-di-*tert*-butyl-*p*-benzoquinone (TBQ), 2,7-dichloro-*p*-benzoquinone (BQ-Cl_2), tetrachloro-*p*-benzoquinone (BQ-Cl_4), *p*-naphthoquinone (*p*-NQ), 2,3-dimethyl-*p*-napthoquinone (*p*-NQ-Me_2), 2,3-dichloro-*p*-napthoquinone (*p*-NQ-Cl_2), 9,10-anthraquinone (AQ), 2-chloro-9,10-anthraquinone (AQ-Cl), ether-derivative of 9,10-anthraquinone (AQ-O-C_3H_7), ester-derivative of 9,10-anthraquinone (AQ-COO-C_3H_7), amide-derivative of 9,10-anthraquinone ((AQ-CONH-C_4H_9), *o*-napthoquinone (*o*-NQ), 9,10-phenanthraquinone (PQ), 2-iodo-9,10-phenanthraquinone (PQ-I), 2,7-diiodo-9,10-phenanthraquinone (PQ-I_2).

The molecular structures of the two classes of quinones, 1,4-cyclohexadienediones (*para*-quinones) and 1,2-cyclohexadienediones (*ortho*-quinones), used in this study are shown in scheme 1. A series of benzoquinones, the simplest class of *para*-quinones, was selected based on their increasing Lewis basicity ranked according to BQ-Cl_4 < BQ-Cl_2 < BQ < TBQ < DBQ as determined by the attached substituents. The electrochemical properties of three *para*-naphthoquinones, benzoquinone derivatives in which an aromatic benzene ring is fused to the C_5-C_6 bond, with basicity increasing in the order *p*-NQ-Cl_2 < *p*-NQ < *p*-NQ-Me_2, were assessed. Anthraquinone is another derivative of benzoquinone, with two aromatic benzene rings fused to the C_2-C_3 and C_5-C_6 bonds, respectively; three derivatives were synthesized in our laboratory to enable comparison of the electrochemistry of their carboxylation reactions with CO_2 with those of the native anthraquinone, AQ. Based on their substituent linking group, the order of increasing Lewis basicity strength is as follows: AQ-COO-C_3H_7 (ester linkage) < AQ-CONH-C_4H_9 (amide linkage) < AQ < AQ-O-C_3H_7 (ether linkage). The four *ortho*-quinones used in our study were *o*-NQ, PQ, PQ-I and PQ-I_2.

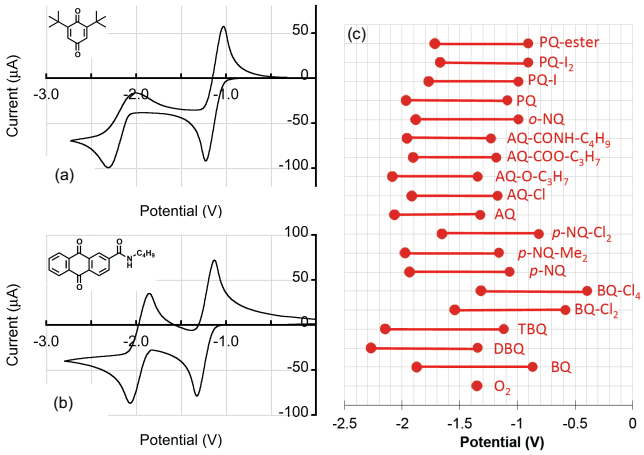

Figure 1: Cyclic voltammetry of 20mM TBQ (a) and 20mM AQ-CONH-C_4H_9 (b) solution of 0.1 M [*n*-Bu_4N]PF_6 in DMF saturated with N_2 at a scan rate of 100mV/s using a platinum electrode. (c) Tabulated cyclic voltammetry results of 20mM solutions of various quinones shown in Scheme 1 in dry 0.1 M [*n*-Bu_4N]PF_6 DMF electrolyte saturated with N_2 at a scan rate of 100 mV/s. The filled symbols represented the half-wave potentials of the first electron transfer from quinones to semiquinones and the second electron transfer, which occurs at more negative electrode potentials, from semiquinones to dianion-quinones. O_2 undergoes quasi-reversible electron transfer forming superoxide, $O_2^{\bullet-}$, in DMF electrolyte solution. The half-wave potential of O_2 is shown.

Figures 1(a) and 1(b) show typical cyclic voltammograms for 2,7-di-*tert*-buty-*p*-benzoquinone (TBQ) in dry dimethylformamide (DMF) electrolyte solutions containing 0.1M [*n*-Bu_4N]PF_6 saturated with N_2, with the first and second half-wave potentials at -1.12 V and -2.15V, respectively (figure 1(a)), and for the amide-derivative 9,10-anthraquinone (AQ-CONH-C_4H_9) with half-wave potentials at -1.23V and -1.96V (figure 1(b)). All potentials were measured using ferrocene as the internal reference. The first wave corresponded to the reduction of quinones, Q, to form semiquinones, $Q^{\bullet-}$, and the second wave reflected the reduction of semiquinones to dianion quinones, Q^{2-}. The first wave was generally reversible while the second wave was at least quasi-reversible. The normal ordering of potentials indicated that the second electron transfer occurred with more difficulty than did the first. This order is expected for quinones in aprotic solvents because the electron transfer to the semiquinone, which already bears a negative charge, requires more energetic electrons to overcome electrostatic repulsions than does the electron transfer to the neutral quinone. Figure 1(c) summarizes the redox potentials for each of the two electron transfers under the same electrolyte conditions as in Figure 1(a) and (b), for the complete set of quinones given in scheme 1. Two consecutive single electron transfers were observed in all cases, with separations in their potentials ranging from 0.72 V to 1.03 V. No complications due to ion-pairing were evident in this work with [*n*-Bu_4N]PF_6 as the supporting electrolyte. Among the *para*-quinones, the potential difference between the first and second electron transfers with benzoquinone was larger than that with naphthoquinone, and the potential difference window for anthraquinone was smaller than that for naphthoquinone. Similarly, PQ showed a smaller potential difference between the first and second electron transfers than did *o*-NQ. The smaller potential differences with larger aromatic structures is because the electric charge on the semiquinones is more delocalized over the larger molecular structures, and thus less energetic electrons are required for the second electron to transfer to these larger structures.

Electrochemistry of weakly complexing quinones in the presence of CO_2

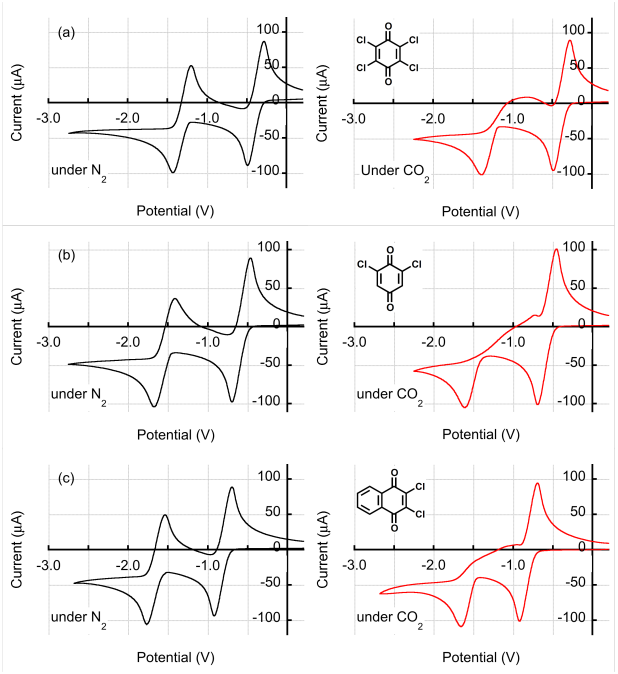

Figure 2: Cyclic voltammetry of 20mM BQ-Cl_4 (a), 20mM BQ-Cl_2 (b), and 20mM *p*-NQ-Cl_2 (c) solution of 0.1 M [*n*-Bu_4N]PF_6 in DMF saturated with N_2 and CO_2 at a scan rate of 100mV/s using a platinum electrode.

Five of the molecules investigated in this study (BQ-Cl_4, BQ-Cl_2, *p*-NQ-Cl_2, AQ-Cl, and AQ-COO-C_3H_7) were categorized as weakly complexing quinones based on the effect their interaction with CO_2 has on their redox properties. A quinone is defined as "weakly complexing" if the corresponding semiquinone shows only weak interaction with CO_2 (small association constant for semiquinone/CO_2 complex).

Figure 2 compares the cyclic voltammograms of three of these quinones under 1 atm N_2 and 1 atm CO_2 atmospheres. In general, when the electrolyte solution was saturated with CO_2, no significant changes were observed in either the cathodic or the anodic waves of the first electron transfer, but the cathodic waves of the second electron transfer were shifted positively, and the oxidation waves exhibited unusual features. In figure 2(a), under N_2 atmosphere, BQ-Cl_4 showed two one-electron transfer processes with the first half-wave potential at -0.39 V and the second at -1.32 V. When CO_2 was introduced to the solution, no changes were observed in the cathodic peak current and position for the first electron transfer, but the second

cathodic wave shifted positively. Oxidation waves in cyclic voltammograms for BQ-Cl_4 showed rather unusual behavior. The first oxidation wave was unusually broad with no distinct peak. The second oxidation wave, at -0.32 V, for BQ-Cl_4, which indicates electron subtraction from the semiquinone to form the neutral quinone was the same for both CO_2- and N_2-saturated DMF electrolyte solutions.

To understand the unusual behavior of the BQ-Cl_4 under a CO_2 atmosphere, we evaluated the electron transfer behavior at different sweep rates (figure 3). Figure 3 shows the cyclic voltammograms for BQ-Cl_4 at sweep rates of 40mV/s, 100mV/s and 200mV/s. At a sweep rate of 40mV/s, the voltammogram showed one oxidation wave from the dianion quinone to form the semiquinone with peak potential at -1.05V. As the sweep rate increased to 100mV/s, this oxidation wave broadened. At a sweep rate of 200mV/s, the voltammogram showed two oxidation waves for the dianion quinone with the first peak potential at -1.05V (A) and the second peak potential at -0.77V (B).

The behavior of weakly complexing quinones like BQ-Cl_4 can be rationalized through the series of equilibrium reactions outlined in Scheme 2a. At the first reduction potential (E_1), quinone is converted to the semiquinone radical anion. For weakly complexing quinones in the presence of CO_2, this species would only weakly interact with CO_2, causing only a minor shift in the second reduction potential compared to that without CO_2. The emergence of two oxidation waves at high scan rates suggests a stronger interaction between the dianion and CO_2, and the existence of two mechanisms for the conversion between semiquinone and CO_2/quinone dianion complexes. Scheme 2a labels these as a *stepwise* and *concerted* process.

Generally, the electrochemical oxidation of a quinone/CO_2 dianion complex would occur at a more positive potential than the oxidation of dianion quinone alone, caused by the extra energy input needed to break the C-O bond. For the *stepwise* process, as we begin to scan the electrode potential towards the positive direction, dianion BQ-Cl_4 will undergo oxidation at the electrode surface first, which decreases the concentration of dianion BQ-Cl_4 within the diffuse layer. In accord with Le Chatelier's principle, more dianion BQ-Cl_4/CO_2 complex would then dissociate to form more dianion BQ-Cl_4 and CO_2. At 40mV/s, the sweep rate of the electrode potential was sufficiently slow to allow the major fraction of dianion BQ-Cl_4/CO_2 complex to dissociate and release CO_2, and to undergo a one-electron oxidation. The *concerted* process would be observed when the sweep rate becomes too fast for mono(carbonate) dianion BQ-Cl_4 to dissociate and keep pace with potential changes (e.g., at 200mV/s). In this case, a significant concentration of dianion BQ-Cl_4/CO_2 complex would be present within the diffuse layer, resulting in an additional oxidation wave at a higher oxidation. At a sweep rate of 200mV/s, the second oxidation wave at -0.77V (labeled as B in Figure 3c) corresponds to the one-electron oxidation of dianion BQ-Cl_4/CO_2 complex to generate semiquinone and CO_2. The oxidation of the bis(carbonate) dianion quinone would also be possible, but for weakly complexing quinones the fraction of bis(carbonate) dianion in solution would be small and thus we anticipate that only oxidation of the mono(carbonate) would be observed. This mechanistic explanation is largely in line with past work,[18,21] but we acknowledge other mechanisms could explain the observed behaviors.

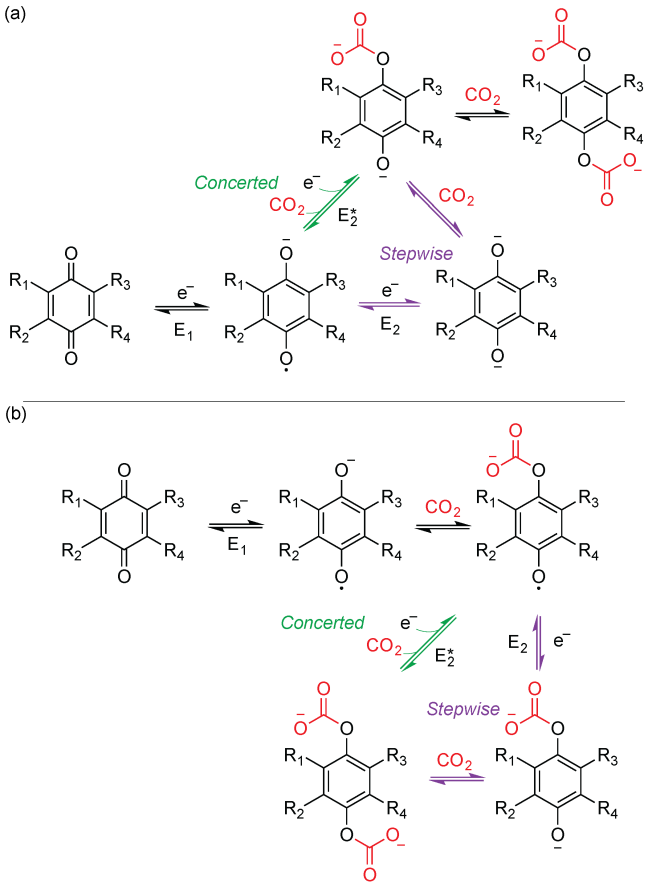

Scheme 2: Proposed mechanism interactions of CO_2 with weakly (a) and strongly (b) complexing quinones during the electrochemical reduction and oxidation processes.

The association constant for the complexation between CO_2 and dianion BQ-Cl_4 was calculated from the positive shift of the half-wave potential of the second-electron transfer when CO_2 was introduced to the solution using the equation

$$K_{b,CO_2}^{app} = \frac{\exp\left(\frac{F}{RT}\Delta E_{Q^{2-}/Q^{\bullet-}}^{\frac{1}{2}}\right)-1}{\left[CO_2\right]^n}$$

where F is the Faraday constant, R is the ideal gas constant, T is the temperature, $\Delta E_{Q^{2-}/Q^{\bullet-}}^{\frac{1}{2}}$ is the shift in the half-wave potentials when CO_2 is introduced to the system, [CO_2] is the concentration of dissolved CO_2, and n is the number of moles of CO_2 per mole of reduced quinones. Assuming one CO_2 is involved in the process, this analysis gives a value of $6.61\times10^2 M^{-1}$ for the CO_2 association constant.

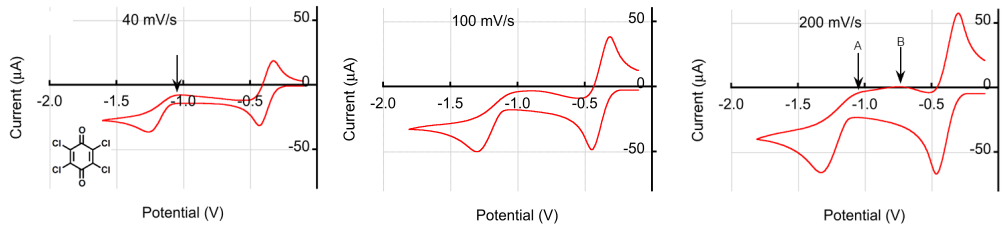

Figure 3: Cyclic voltammetry of 10mM BQ-Cl_4 solutions of 0.1 M [*n*-Bu_4N]PF_6 in DMF saturated with CO_2 at sweep rates of 40 mV/s, 100 mV/s and 200 mV/s using a platinum electrode. Arrows highlight observed oxidation waves.

Similarly, BQ-Cl_2 and *p*-NQ-Cl_2 underwent two one-electron transfers under an N_2 atmosphere, with a positive shift in the second electron transfer potential under CO_2 (figure 2(b) and 2(c)). The CO_2 association constants with the BQ-Cl_2 and *p*-NQ-Cl_2 dianions are $8.18\times10^5 M^{-1}$ and $7.32\times10^4 M^{-1}$, respectively. The variations in the CO_2 association constants for BQ-Cl_2, BQ-Cl_4 and *p*-NQ-Cl_2 are due to the resonance stabilization of the oxyanion through the inductive effects of functional groups conjugated to the quinoid ring-structures. A greater stabilization of the oxyanion lowers its nucleophilic reactivity towards CO_2 addition and decreases the CO_2 association constant. The decrease in CO_2 binding constant for *p*-NQ-Cl_2 over the BQ-Cl_2 dianion, for instance, was due mainly to the resonance stabilization through electron delocalization within the aromatic phenyl groups fused to the quinone ring-structure, consistent with the effect of resonance stabilization on the basicity of aromatic oxide anions observed in phenol and 1-naphthol molecules. In a dilute aqueous solution, the protonated phenol, the phenoxide anion (pK_b = 3.11), is more basic than the protonated 1-naphthol (pK_b = 3.66).[24] In organic solvents, the strength of an oxyanion Lewis base is reflected in its hydrogen-bonding power. The observations of Ahmed *et al*. that the oxyanions of naphthoquinones are weaker hydrogen-bonding acceptors than those of benzoquinones also support our experimental results showing weaker CO_2 binding to fused ring substituted quinones.[25] The lower CO_2 binding constant for BQ-Cl_4 as compared to BQ-Cl_2 is predominantly due to the electron-withdrawing character of the chlorine side groups; replacement of the two hydrogen atoms of BQ-Cl_2 with two chlorine atoms allows for greater stabilization of the dianion BQ-Cl_4 and a decrease in the nucleophilicity of this anion toward CO_2. The asymmetry of BQ-Cl_2 may also contribute to this difference.

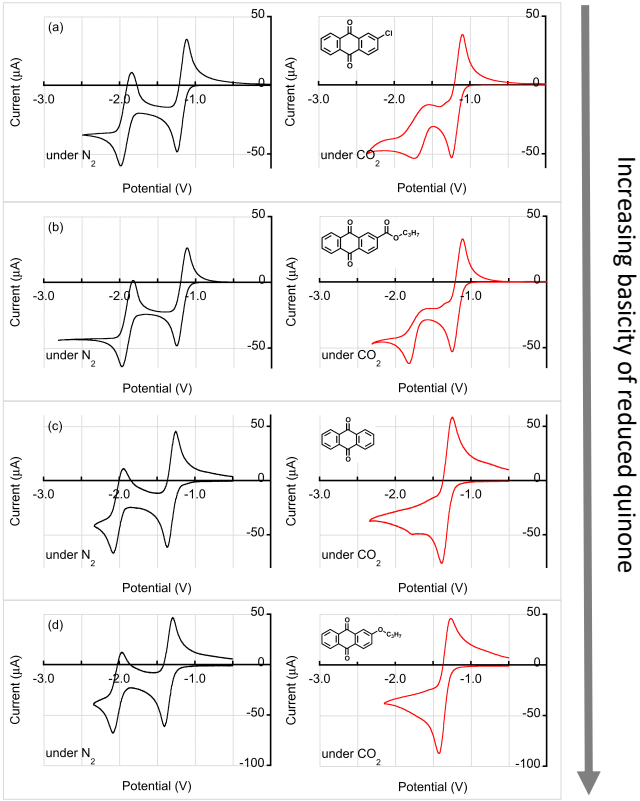

Figure 4: Cyclic voltammetry of AQ-Cl (a), AQ-COO-C_3H_7 (b), AQ (c) and AQ-O-C_3H_7 (d,) solutions of 0.1 M [*n*-Bu_4N]PF_6 in DMF saturated with either N_2 (black waves) or CO_2 (red waves) at a scan rate of 100mV/s using a platinum electrode.

Fusion of the aromatic phenyl group to the quinone ring showed less of an effect on the resonance stabilization of the oxyanions than did conjugation of the electron-withdrawing groups to the quinone-ring structure. Thus, replacement of the electron-withdrawing groups with fused aromatic phenyl groups increases the CO_2 association constant, as demonstrated for the anthraquinone derivatives, AQ-Cl and AQ-COO-C_3H_7, which we categorized as weakly complexing quinones (figure 4(a) and 4(b)). The first CO_2 association constants of AQ-Cl and AQ-COO-C_3H_7 were $2.35\times10^5 M^{-1}$ and $7.78\times10^7 M^{-1}$, respectively. Among the weakly complexing quinones investigated, AQ-COO-C_3H_7 showed the highest CO_2 association constants.

Electrochemistry of strongly complexing quinones in the presence of CO_2

Addition of CO_2 to quinones that interact strongly with the CO_2 led to very different cyclic voltammetric waves than those discussed for weakly complexing quinones. Eleven compounds from the list of quinones in scheme 1 were categorized as strongly complexing quinones; these were BQ, *p*-NQ, AQ, AQ-O-C_3H_7, *o*-NQ, PQ, DBQ, TBQ, *p*-NQ-Me_2, PQ-I and PQ-I_2. In the discussions that follow, we focus on the first six compounds as these quinones presented unique cyclic voltammograms over the complete interaction range.

The anthraquinone derivative, AQ-COO-C_3H_7, showed the strongest CO_2 association constant among the group of weakly complexing quinones. The electron-withdrawing nature of the carbonyl group (C=O) of the ester linkage lowers the Lewis basicity of the oxyanion, which limits its association constant with CO_2. Replacing the ester linkage with any electron-releasing substituent results in an increase in the CO_2 association constant. The electrochemical behavior of two anthraquinone derivatives with two opposite inductive effects, AQ-COO-C_3H_7 and AQ-O-C_3H_7, was compared with that of the original anthraquinone molecules, AQ, for which the inductive effect of the hydrogen is between that of the carbonyl and the ether linkages (figure 4).

In dry DMF electrolyte saturated with N_2, cyclic voltammograms of AQ-COO-C_3H_7, AQ and AQ-O-C_3H_7 showed two one-electron transfer waves, which were separated by about 0.7V (figure 4(b), (c) and (d)). As with other weakly complexing quinones, there was no change in the peak current and position of the first reduction wave for AQ-COO-C_3H_7 when the electrolyte solution was saturated with CO_2 but the second reduction wave was shifted positively (figure 4(b)). With both hydrogen and the ether linkage, the CO_2 association constant was expected to be stronger than with the ester linkage, and accordingly we observed larger positive shifts of the second reduction waves for AQ and AQ-O-C_3H_7 (figure 4(c) and (d)). The positive shift of the second reduction wave was accompanied by an increase in the first cathodic current. The second reduction wave was almost lost in the case of AQ (figure 4(c)) and only a shoulder was observed in the case of AQ-O-C_3H_7 (figure 4(d)). The first cathodic peak current of AQ increased from 56µA to 70 µA, while the cathodic peak current for AQ-O-C_3H_7 increased from 56 µA to 83µA. Only one oxidation wave was observed in the voltammograms of AQ and AQ-O-C_3H_7 with the current of the oxidation wave under CO_2 higher than that under N_2.

For these strongly complexing quinones, the ECE mechanism proposed initially by Mizen and Wrighton is operative.[9] We label this process the *stepwise* mechanism in Scheme 2b. The mechanism of the carbonate formation is initially by a one-electron reduction of the neutral quinone to form a semiquinone that then complexes with CO_2. These intermediate complexes immediately undergo the second one-electron reduction in close proximity to the electrode surface to form the mono(carbonate) of the dianion quinone, which can subsequently complex with another CO_2 to yield quinone bis(carbonate). The CO_2 association constants for AQ and AQ-O-C_3H_7 could not be obtained from cyclic voltammograms because we were not able to deduce the half-wave potential of the second electron transfer. The only conclusion was thus that the CO_2 association constants for AQ and AQ-O-C_3H_7 are greater than the association constant of about 10^8 M^{-1} for AQ-COO-C_3H_7.

Quinones with electron-releasing substituent groups attached to their rings are expected to have stronger CO_2 association constants. Based on their molecular structures, the oxyanions of BQ and *p*-NQ should have CO_2 association constants higher than those of both AQ and AQ-O-C_3H_7. With the concept of resonance stabilization and its effects on the basicity of aromatic oxyanions described previously, the basicity of *p*-NQ oxyanion is expected to be between those of BQ and AQ. With no fused aromatic phenyl ring, the BQ oxyanion is the strongest Lewis base among these three quinones.

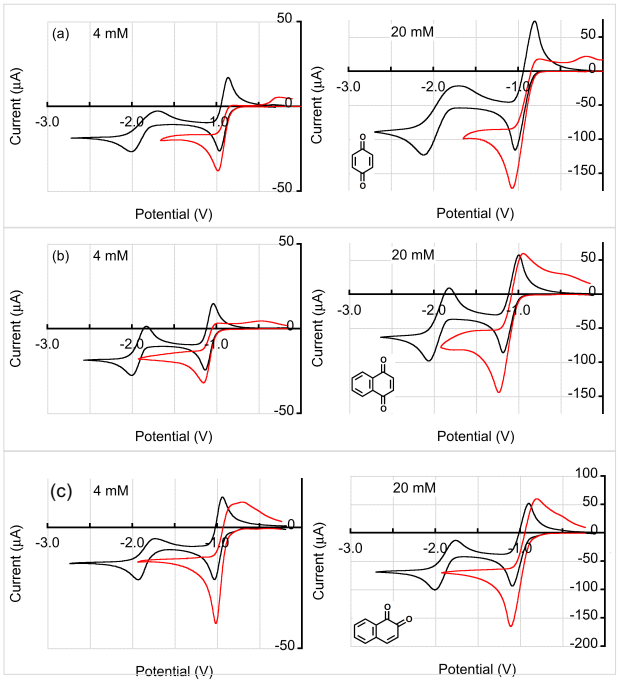

Figure 5: Cyclic voltammetry of BQ (a), *p*-NQ (b), and *o*-NQ (c) solutions of 0.1 M [*n*-Bu_4N]PF_6 in DMF saturated with either N_2 (grey waves) or CO_2 (red waves) at a scan rate of 100mV/s using a platinum electrode.

Two well-separated electrochemical waves were observed for BQ and *p*-NQ solutions under an N_2 environment (figure 5(a) and (b), grey lines). In the presence of CO_2 these quinones showed a significant increase in the peak current of the first electron transfer, attributed to two consecutive electron transfers at this reduction wave potential, and the disappearance of the reduction wave of the second electron transfer (figure 5(a) and (b), red lines), according to the ECE mechanism.

Quinones exist in two isomeric forms, 1,4-cyclohexadienedione (*para*-quinone) and 1,2-cyclohexadienedione (*ortho*-quinone). In dilute aqueous solution, the deprotonated hydroquinone (pK_b = 3.65) is more basic than the deprotonated catechol (pK_b = 4.15); therefore we expect that dianions of *ortho*-quinones will be less basic than those of *para*-quinones.[22] As shown in figure 5(c), the reduction potential of *o*-NQ is slightly

more positive than that of *p*-NQ. For *o*-NQ, the potential separation between the two reduction peaks under N_2 is about 0.89 V, slightly wider than that of *p*-NQ, 0.87 V. The larger potential separation with *ortho*-quinones is because, due to their close proximity, the two oxyanions in C_1 and C_2 positions experience larger electrostatic repulsion.

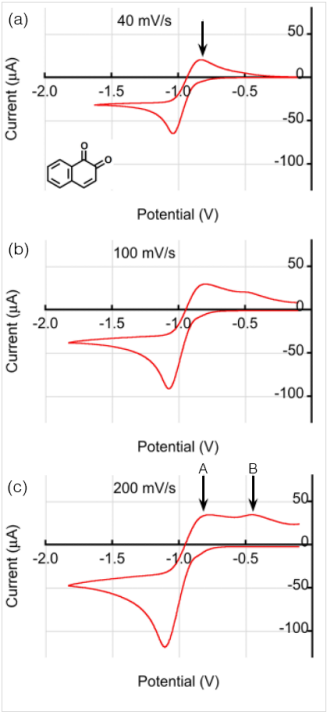

Figure 6: Cyclic voltammetry of 10mM *o*-NQ in 0.1 M [*n*-Bu_4N]PF_6 DMF electrolyte saturated with CO_2 at sweep rates of 40 mV/s, 100 mV/s and 200 mV/s using a platinum electrode. Arrows highlight observed oxidation waves.

AQ and its derivatives in the presence of CO_2 only exhibited an oxidation wave that coincided with the single reduction wave (figure 4) at 100 mV/s. As opposed to the voltammograms for AQ and AQ derivatives, those for BQ, p-NQ, and o-NQ revealed two oxidation waves at 100 mV/s in the presence of CO_2 (figure 5, red lines), corresponding to two different oxidation mechanisms at the two oxidation potentials. At lower concentration (4 mM, left panels), the first wave that coincides with the single reduction wave is reduced in size. We attribute the first oxidation wave to oxidation of mono(carbonate) quinone dianion, and the second, which occurred at a less negative potential, to the oxidation of bis(carbonate) quinone dianion. Scheme 2b labels these as *stepwise* and *concerted* mechanisms, respectively. An equilibrium would exist between the mono(carbonate) dianion and the bis(carbonate) dianion. As the electrode potential is swept to less negative values, the mono(carbonate) dianion would first be oxidized, shifting the equilibrium to release CO_2 and generate additional mono(carbonate) which would subsequently be oxidized. At low quinone concentration, the CO_2 would be in excess and bis(carbonate) dianion would primarily exist. For stronger binding quinones, the equilibrium would also be driven towards the bis(carbonate) form. The oxidation of uncomplexed dianion would also be possible, but with sufficient CO_2 this species should contribute only minimally to the observed voltammogram. These arguments are consistent with the trends between BQ, p-NQ, and o-NQ in figure 5, where o-NQ would have the lowest binding strength and thus exhibits a larger wave associated with oxidation of the mono(carbonate) quinone. Varying the scan rate for o-NQ (figure 6) demonstrated the emergence of a second oxidation wave at higher potential (labeled B in Figure 6c), which would occur if the equilibrium described did not have time to fully equilibrate before a potential energetic enough to oxidize the bis(carbonate) was reached. We note that some groups have noted the potential for additional side reactions with BQ given the possibility of addition to the neighboring carbons,[22] and that alternative mechanistic interpretations may be possible.

Considerations on practical implementation of capture with quinones

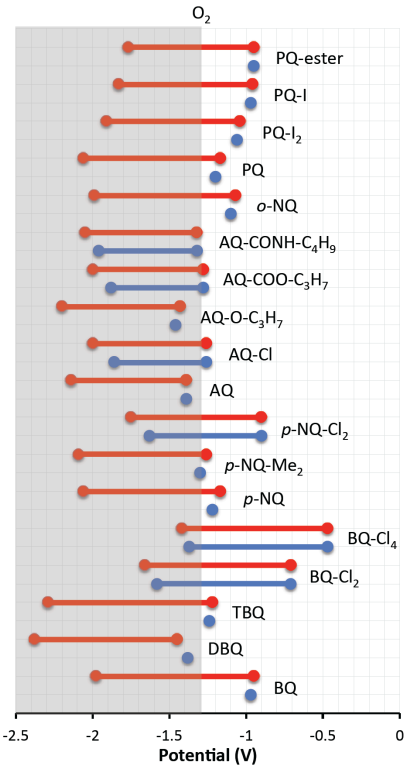

Figure 7: Tabulated cyclic voltammetric results of 20mM solution of various quinones shown in **Scheme 1** in dry 0.1 M [*n*-Bu_4N]PF_6 DMF electrolyte saturated with either N_2 (red symbol) or CO_2 (blue symbol) at a scan rate of 100 mV/s. The filled symbols represented the half-wave potentials of the first electron transfer from quinones to semiquinones and the second electron transfer, which occurs at more negative electrode potential, from semiquinones to dianion-quinones.

The systematic study presented in this work indicates a range of potential quinones for application in selective CO_2 concentration from dilute gas and should serve as a useful reference for many future studies. There are a number of potential issues to consider in practical applications, however. First is the possibility of parasitic reactions between reduced quinones and oxygen. In a dry DMF electrolyte solution, O_2 showed a quasi-

reversible electron transfer to form the superoxide with a half-wave potential of -1.3 V.[26] For CO_2 electrochemical concentrators, this reaction will decrease the overall efficiency of the process. The peak potentials of the reduction waves under N_2 and CO_2 for the various quinone structures studied are summarized in figure 7, relative to the reduction potential of O_2.

The weakly complexing quinones showed CO_2 association constants in the range of 10^2 M^{-1} to $10^7 M^{-1}$, and could potentially be used for CO_2 separation; however, during the CO_2 capture step, these quinones need to be activated electrochemically to form dianion quinones with electrode potentials ranging from -1.32 V to -1.96 V. With this range of activation potentials, the formation of superoxide along with the generation of the dianion quinones on the electrode is unavoidable if oxygen is present. Therefore, the weakly complexing quinones are not suitable candidates for CO_2 separation from dilute gas effluents that contain O_2. While the two reduction waves and larger negative electrode potentials required for the carboxylation of weakly-complexing quinones mitigate against their use as complexing agents in CO_2 capture applications, this is not the case for the strongly complexing quinones, which exhibited adequate redox characteristics for the effective separation of CO_2 from gas mixtures in the presence of O_2. During the capture step, these compounds can be activated electrochemically to form semiquinones with electrode potentials ranging from -0.87 V to -1.07 V, and can subsequently capture a second CO_2, as previously discussed. These potentials are more positive than the -1.3V at which the undesirable superoxide anion forms on the electrode.

This discussion applies to DMF, though similar considerations will also be necessary for other solvents. DMF has a large vapor pressure and would not be practical for implementation at scale. Instead, solvents with a low vapor pressure including ionic liquids that we have previously reported on would be necessary.[10] As discussed in this prior work, the chosen solvent requires low viscosity, a high resistance to foam or mist formation, a relatively low solubility of CO_2 to limit carry over, and a large quinone solubility.

The development of electrochemical CO_2 separation strategies for the next generation capture facilities at fossil fuel burning facilities, cement plants, or steel plants must consider the effects of other components in the flue gas emissions, especially those of the acidic gases such as sulfur and nitric oxides. It should also be noted that other degradation mechanisms may be possible with oxygen. The effects of such flue gas components on the electrochemistry and stability of quinones is an active area of research.

Conclusion

A comprehensive potentiometric assessment of the effects of interactions of CO_2 with quinones in dry DMF electrolyte solutions under reducing and oxidizing conditions was performed. In N_2 saturated aprotic electrolyte solutions, the quinones undergo two consecutive electron transfers with the first electron transfer exhibiting reversible, and the second quasi-reversible behavior. Under a CO_2 saturated environment, the carboxylation of the dianion quinones to form C-O covalent bonds induces irreversibility in the second electron transfer at the sweep rates used. The thermodynamic association constants of CO_2 with different quinones vary with their molecular structures; two different classes of quinones were identified, i.e. weakly- and strongly-complexing quinones. For the weakly complexing quinones, BQ-Cl_4, BQ-Cl_2, *p*-NQ-Cl_2, AQ-COO-C_3H_7 and AQ-CONH-C_4H_9, two well-separated reduction waves were observed in CO_2 saturated aprotic electrolyte solutions with no change in the position of the first reduction peak and a positive shift of the second reduction peak. Two anodic current peaks were observed for the dissociation of the dianion quinone-CO_2 complexes, corresponding to *step-wise* oxidation and *concerted* oxidation of these complexes. For the strongly-complexing quinones, BQ, TBQ, DBQ, *p*-NQ, *p*-NQ-Me_2, AQ, AQ-O-C_3H_7, *o*-NQ and PQ, the voltammograms featured an increase in the first reduction peak current and the disappearance of the second reduction and oxidation waves. It was inferred that their semiquinones associated with CO_2 to form intermediate complexes that subsequently experienced the second electron transfer at the same or almost the same reduction potential as that at which the first electron transferred. For BQ, p-NQ, and o-NQ, two anodic peak currents were observed and identified as being due to the oxidations of the mono(carbonate) and bis(carbonate), respectively, of the dianion quinone-CO_2 complexes. The potentials of the second anodic peak current were dependent on the quinone molecular structure and quinone concentration. Overall, the correlation between quinone structure and the association constant for its binding with CO_2 was assessed, and the possible mechanisms of the oxidations of the dianion quinone-CO_2 complexes were inferred.

Optimization of the electrode potentials at which the quinones are activated to complex with CO_2 (reduction) and deactivated to release the CO_2 (oxidation) is important for the design and operation of energy-efficient CO_2 electrochemical separators for potential use on the gaseous emissions from fossil fuel-fired facilities and other industrial sources such as the steel and cement industries, and from mobile sources such as vehicles, boats and trains, as well as in the reduction of CO_2 concentrations directly from the ambient air or from confined spaces such as buildings, submarines, and spacecraft. We have identified a number of quinoidal compounds that have the desired operational ranges and whose reduction potentials are sufficiently more positive than that of oxygen so that the formation of the undesirable superoxide anion can be avoided during the electrochemical swing operations. Other acidic gases such as sulfur and nitrogen oxides are also often present in the emissions, albeit in trace quantities relative to the CO_2, and their impact on the effectiveness of any process using these systems must be considered in the design and implementation of new separation technologies. This work should inform the future rational design of electrochemical CO_2 separators.

Experimental section

Materials: *p*-benzoquinone (BQ), tetramethyl-*p*-benzoquinone (DBQ), 2,7-di-*tert*-butyl-*p*-benzoquinone (TBQ), 2,7-dichloro-*p*-benzoquinone (BQ-Cl_2), tetrachloro-*p*-benzoquinone (BQ-Cl_4), 2,3-dimethyl-*p*-napthoquinone (*p*-NQ-Me_2), anhydrous dimethylformamide (DMF), tetrabutylammonium hexafluorophosphate ([*n*-Bu_4N]PF_6), potassium permanganate ($KMnO_4$), glacial acetic acid (AcOH), acetic anhydride (Ac_2O), sodium sulfite (Na_2SO_3), ammonium carbonate (NH_4CO_3), sulphuric acid, diiodine, toluene, methanol, 1-bromopropane, butylamine were purchased from Sigma-Aldrich®. *p*-napthoquinone (*p*-NQ), 2,3-dichloro-*p*-napthoquinone (*p*-NQ-Cl_2), 9,10-anthraquinone (AQ), 2-chloro-9,10-anthraquinone (AQ-Cl), *o*-napthoquinone (*o*-NQ), 9,10-phenanthraquinone (PQ), 2-hydroxy-9,10-anthraquinone (AQ-OH), 2-carboxylic acid-9,10-antraquinone (AQ-COOH) were purchased from TCI America. All chemicals were used as received without purification.

Synthesis of ether-derivative of 9,10-anthraquinone (AQ-O-C_3H_7): AQ-OH and 1-bromopropane, together with sodium hydroxide were stirred in DMF at 80°C until TLC indicated full conversion, about 1 h. The reaction mixture was cooled and filtrated, the solid was with acetone. The amount of DMF was reduced by partial evaporation and the concentrated solution was precipitated in a 1N HCl solution. The product was extracted with dichloromethane. Pure product was obtained after recrystallization from methanol.

Synthesis of ester-derivative of 9,10-anthraquinone (AQ-COO-C_3H_7): AQ-COOH and 1-bromopropane, together with sodium hydroxide were stirred in DMF at 80°C until TLC indicated full conversion, about 1 h. The reaction mixture was cooled and filtrated, the solid was with acetone. The amount of DMF was reduced by partial evaporation and the concentrated solution was precipitated in a 1N HCl solution. The product was extracted with dichloromethane. Pure product was obtained after recrystallization from methanol.

Synthesis of 2-iodo-9,10-phenanthraquinone (PQ-I) and 2,7-diiodo-9,10-phenanthraquinone (PQ-I_2): The procedure was modified and optimized from the previous work by Lulinski P. and Skulski L.[27] Powdered $KMnO_4$ was suspended in a mixture of AcOH with Ac_2O cooled under ice bath. Diiodine was added, and concentrated sulphuric acid was slowly added dropwise with stirring and keeping the temperature below 5°C. PQ was added, and the whole was stirred for 6 h at 50°C. The reaction mixture was poured, with stirring, into ice-water containing the previously dissolved Na_2SO_3 and $(NH_4)_2CO_3$. The solid products were collected by filtration, washed well with deionized water until the washing were colorless and neutral, and air-dried. The products were separated with column chromatography with mixture of toluene and ethyl acetate as the mobile phase.

Electrochemical experiment: Cyclic voltammetry measurements were carried out with a standard three-electrode cell using an VersaSTAT 3 potentiostat with Versa studio software from Princeton applied research. Electrochemical measurements were conducted in a glass cell, thermostated at defined temperatures. The platinum-working electrode was purchased from BASi corporate. Platinum wire served as the counter electrode and Ag/AgCl wire served as the reference electrode. Ferrocene was used as the internal standard. DMF containing 0.1 M [*n*-Bu_4N]PF_6 was used as an electrolyte. The solution was carefully deoxygenated with nitrogen with gentle stirring for 30 min and the nitrogen atmosphere was maintained during the electrochemical experiments. To test the electrochemical behavior of quinones under CO_2, the electrolyte was bubbled with 100% CO_2 for 30 min before testing.

AUTHOR INFORMATION

Corresponding Author

* Email: tahatton@mit.edu.

Funding Sources

This work is supported by the Innovative Materials and Processes for Advanced Carbon Capture Technologies (IMPACCT) program of Advanced Research Project Agency-Energy (ARPA-E) (grant DE-AR0000083).

ACKNOWLEDGMENT

We thank Dr. Renu Ravindranath for fruitful discussion on electrochemical experiments and chemical synthesis. We acknowledge support from Siemens Corporate Research team in Erlangen, Germany, specifically Dr. Thomas Hammer and Dr. Harald Landes. We gratefully acknowledge financial support from Siemens CKI research fund and ARPA-E research grant, DE-AR0000083.

ABBREVIATIONS

CCS, Carbon Capture and Sequestration; DMF, dimethylformamide; ECE, Electrochemical Chemical Electrochemical reactions.

REFERENCES

(1) Rochelle, G. T. Amine Scrubbing for CO_2 Capture. *Science* 2009, *325* (5948), 1652–1654.

(2) Rheinhardt, J. H.; Singh, P.; Tarakeshwar, P.; Buttry, D. A. Electrochemical Capture and Release of Carbon Dioxide. *ACS Energy Lett.* 2017, *2* (2), 454–461.

(3) Sharifian, R.; Wagterveld, M.; Digdaya, I. A.; Xiang, C.; Vermaas, D. A. Electrochemical Carbon Dioxide Capture to Close the Carbon Cycle. *Energy Environ. Sci.* 2021, *10* (3), 147–154.

(4) Renfrew, S. E.; Starr, D. E.; Strasser, P. Electrochemical Approaches toward CO_2 Capture and Concentration. *ACS Catal.* 2020, *10* (21), 13058–13074.

(5) Kang, J. S.; Kim, S.; Hatton, T. A. Redox-Responsive Sorbents and Mediators for Electrochemically Based CO_2 Capture. *Curr. Opin. Green Sustain. Chem.* 2021, 100504.

(6) Mizen, M. B.; Wrighton, M. S. Reductive Addition of CO_2 to 9,10-Phenanthrenequinone. *J. Electrochem. Soc.* 1989, *136* (4), 941.

(7) Dubois, D. L.; Miedaner, A.; Bell, W.; Smart, J. C. Electrochemical Concentration of Carbon Dioxide. In *Electrochemical and Electrocatalytic Reactions of Carbon Dioxide*; Sullivan, B. P., Ed.; Elsevier, 1993; p iii.

(8) Scovazzo, P.; Poshusta, J.; DuBois, D.; Koval, C.; Noble, R. Electrochemical Separation and Concentration of <1% Carbon Dioxide from Nitrogen. *J. Electrochem. Soc.* 2003, *150* (5), D91.

(9) Voskian, S.; Hatton, T. A. Faradaic Electro-Swing Reactive Adsorption for CO_2 Capture. *Energy Environ. Sci.* 2019, *12* (12), 3530–3547.

(10) Gurkan, B.; Simeon, F.; Hatton, T. A. Quinone Reduction in Ionic Liquids for Electrochemical CO_2 Separation. *ACS Sustain. Chem. Eng.* 2015, *3* (7), 1394–1405.

(11) Liu, Y.; Ye, H.; Diederichsen, K. M.; Van Voorhis, T.; Hatton, T. A. Electrochemically Mediated Carbon Dioxide Separation with Quinone Chemistry in Salt-Concentrated Aqueous Media. *Nat. Commun.* 2020, *11* (1), 2278.

(12) Stern, M. C.; Simeon, F.; Hammer, T.; Landes, H.; Herzog, H. J.; Hatton, T. A. Electrochemically Mediated Separation for Carbon Capture. *Energy Procedia* 2011, *4*, 860–867.

(13) Gupta, N.; Linschitz, H. Hydrogen-Bonding and Protonation Effects in Electrochemistry of Quinones in Aprotic Solvents. *J. Am. Chem. Soc.* 1997, *119* (27), 6384–6391.

(14) Hui, Y.; Chng, E. L. K.; Chng, C. Y. L.; Poh, H. L.; Webster, R. D. Hydrogen-Bonding Interactions between Water and the One- and Two-Electron-Reduced Forms of Vitamin K 1 : Applying Quinone Electrochemistry To Determine the Moisture Content of Non-Aqueous Solvents. *J. Am. Chem. Soc.* 2009, *131* (4), 1523–1534.

(15) Quan, M.; Sanchez, D.; Wasylkiw, M. F.; Smith, D. K. Voltammetry of Quinones in Unbuffered Aqueous Solution: Reassessing the Roles of Proton Transfer and Hydrogen Bonding in the Aqueous Electrochemistry of Quinones. *J. Am. Chem. Soc.* 2007, *129* (42), 12847–12856.

(16) Ge, Y.; Lilienthal, R. R.; Smith, D. K. Electrochemically-Controlled Hydrogen Bonding. Selective Recognition of Urea and Amide Derivatives by Simple Redox-Dependent Receptors. *J. Am. Chem. Soc.* 1996, *118* (16), 3976–3977.

(17) De Sousa Bulhões, L. O.; Zara, A. J. The Effect of Carbon Dioxide on the Electroreduction of 1,4-Benzoquinone. *J. Electroanal. Chem. Interfacial Electrochem.* 1988, *248* (1), 159–165.

(18) Nagaoka, T.; Nishii, N.; Fujii, K.; Ogura, K. Mechanisms of Reductive Addition of CO_2 to Quinones in Acetonitrile. *J. Electroanal. Chem.* 1992, *322* (1–2), 383–389.

(19) Comeau Simpson, T.; Durand, R. R. Reactivity of Carbon Dioxide with Quinones. *Electrochim. Acta* 1990, *35* (9), 1399–1403.

(20) Tanaka, H.; Nagao, H.; Tanaka, K. Evaluation of Acidity of CO_2 in Protic Media. Carboxylation of Reduced Quinone. *Chem. Lett.* 1993, *22* (3), 541–544.

(21) Namazian, M.; Zare, H. R.; Yousofian-Varzaneh, H. Electrochemical Behavior of Tetrafluoro-p-Benzoquinone at the Presence of Carbon Dioxide: Experimental and Theoretical Studies. *Electrochim. Acta* 2016, *196*, 692–698.

(22) Fan, H.; Cheng, L.; Jin, B. Investigation on Electrochemical Capture of CO_2 in p-Benzoquinone Solutions by in Situ FT-IR Spectroelectrochemistry. *Electrochim. Acta* 2019, *324*, 134882.

(23) Tam, S. M.; Tessensohn, M. E.; Tan, J. Y.; Subrata, A.; Webster, R. D. Competition between Reversible Capture of CO_2 and Release of $CO_2^{\bullet-}$ Using Electrochemically Reduced Quinones in Acetonitrile Solutions. *J. Phys. Chem. C* 2021, *125* (22), 11916–11927.

(24) Perrin, D.; Dempsey, B.; Serjeant, E. P. *PKa Prediction for Organic Acids and Bases*; Chapman & Hall: London, 1981.

(25) Ahmed, S.; Khan, A. Y.; Qureshi, R. Electrochemical Study of Hydrogen-Bonding in Anthraquinones. *J. Chem. Soc. Pakistan* 2006, *28* (6), 542–548.

(26) Jain, P. S.; Lal, S. Electrolytic Reduction of Oxygen at Solid Electrodes in Aprotic Solvents-the Superoxide Ion. *Electrochim. Acta* 1982, *27* (6), 759–763.

(27) Lulinski, P.; Skulski, L. Oxidative Iodination of Arenes with Manganese(IV) Oxide or Potassium Permanganate as the Oxidants. *Bull. Chem. Soc. Jpn.* 1999, *72* (1), 115–120.